

# Estimation of the Radio Channel Parameters using the SAGE Algorithm

Susana MOTA<sup>1</sup>, Maura OUTEIRAL GARCIA<sup>2</sup>, Armando ROCHA<sup>1</sup>, Fernando PEREZ-FONTAN<sup>2</sup>

<sup>1</sup> Dept. of Electronics, Telecommunications and Informatics, Instituto de Telecomunicações, University of Aveiro  
Campus Universitário de Santiago, 3800 – 193 Aveiro, Portugal

<sup>2</sup> Dept. of Signal Theory and Communications, University of Vigo, 36310 Vigo, Spain

smota@ua.pt, mau.outeiral@ua.pt, arocha@av.it.pt, fpfontan@tsc.uvigo.es

**Abstract.** *This paper presents the problem of estimating the parameters of a given number of superimposed signals, as is the case of the received signal in wireless communications. Based on the description of the received signal in the frequency domain, one version of the SAGE (Space-Alternating Generalized Expectation-Maximization) algorithm is presented, allowing the estimation, for each impinging ray, the delay, azimuth, elevation and complex amplitude. Ray retrieval results are presented in synthetic channels, using data generated with the extended Saleh-Valenzuela (ESV) model, and also in real channels.*

## Keywords

Parameter estimation, SAGE algorithm, radio channel measurements, multipath components.

## 1. Introduction

Research, design and analysis of advanced wireless communications systems require a detailed understanding of the electromagnetic wave propagation phenomena in mobile radio environments. System performance evaluation yields representative results only if the underlying channel models reflect the most relevant features of the physical channel. An important effort has been devoted to the channel's directional information: how many are the most important waves arriving at the antenna, from where and with what amplitude and delays do they come [1], [2], [3]. The development of these new channel models relies on a realistic characterization of the probability distribution of several parameters, requires extensive measurements on a wide range of scenarios and validation against theoretical predictions. Therefore, suitable and computationally efficient processing tools need to be employed in order to extract the parameters of interest from the measured data.

A few high-resolution algorithms have been proposed and used to estimate the parameters of the impinging

waves in mobile radio environments. In particular, the SAGE (Space-Alternating Generalized Expectation-Maximization) algorithm simplifies the complex multi-dimensional optimization problem, such as estimating the parameters of these waves in a multipath propagation environment, to several separate one-dimensional optimization processes which can be performed sequentially. This algorithm, derived in its general form in [4], is an extension to the Expectation-Maximization (EM) algorithm [5] and has been used in areas like image reconstruction [6].

In the context of array signal processing, comparative convergence studies of the EM and SAGE algorithms applied to Angle of Arrival (AoA) estimation may be found in [7] using synthetic data, and in [8] using measured sonar data. Concerning the wireless communications context, the SAGE algorithm has been used for joint delay, azimuth and Doppler frequency estimation in time-variant channels [9], [10], as well as, for joint delay, azimuth and elevation estimation in time-invariant channels [11], [12].

In this work, we present one version of the SAGE algorithm in the frequency domain, allowing the estimation of the delay, azimuth, elevation and complex amplitude for a given number of superimposed electromagnetic waves. Estimation accuracy and reliability is investigated using both synthetic and measured data.

The paper is organized as follows. To start, in Section 2, some definitions, notations and the signal and channel models are established. Then, in Section 3, EM based estimation and the SAGE algorithm are presented. Ray retrieval results in synthetic channels and also in real channels appear, respectively, in Section 4 and Section 5. Finally in Section 6 the conclusions are presented.

## 2. Signal Model

In the considered underlying model [12], a finite number,  $L$ , of plane waves are impinging at the receiver antenna array with  $M$  elements and the channel is assumed time-invariant. The channel impulse response at the  $m^{\text{th}}$  antenna element can be expressed as

$$h_m(t, \phi, \beta) = \sum_{\ell=1}^L \alpha_\ell \exp\left(j \frac{2\pi}{\lambda} \langle r_m, e(\phi_\ell, \beta_\ell) \rangle\right) \delta(t - \tau_\ell) \quad (1)$$

where:  $\tau_\ell$  represents the time delay,  $\phi_\ell$  the incidence azimuth,  $\beta_\ell$  the incidence elevation (measured with respect to the horizontal plane) and  $\alpha_\ell$  the complex amplitude of the  $\ell$ -th wave;  $\lambda$  denotes the wavelength and  $\langle \cdot, \cdot \rangle$  the scalar product;  $r_m$  is a row vector containing the  $m$ -th antenna element coordinates and

$$e(\phi, \beta) = [\cos \beta \cos \phi, \cos \beta \sin \phi, \sin \beta]^T \quad (2)$$

is the unit vector in  $\mathbb{R}^3$  pointing toward the direction defined by  $\phi$  and  $\beta$ , where  $[ \cdot ]^T$  denotes matrix transposition.

In (1), the expression

$$c_m(\phi_\ell, \beta_\ell) = \exp\left(j \frac{2\pi}{\lambda} \langle r_m, e(\phi_\ell, \beta_\ell) \rangle\right) \quad (3)$$

accounts for the phase shift suffered by the  $\ell^{\text{th}}$  wave due to a small difference in the traveled distance to reach the  $m^{\text{th}}$  antenna element. The vector

$$c(\phi, \beta) = [c_1(\phi, \beta), \dots, c_M(\phi, \beta)]^T \quad (4)$$

is the so called array steering vector.

Defining  $\theta_\ell = [\tau_\ell, \phi_\ell, \beta_\ell, \alpha_\ell]$  as being the vector which contains the parameters of the  $\ell$ -th wave, the contribution of this wave to the  $M$  impulse responses may be expressed as

$$h(t; \theta_\ell) = [h_1(t; \theta_\ell), \dots, h_M(t; \theta_\ell)]^T = \alpha_\ell c(\phi_\ell, \beta_\ell) \delta(t - \tau_\ell). \quad (5)$$

Alternatively, in the frequency domain, the channel transfer matrix across the array, possibly corrupted with noise is given by

$$H(f; \theta) = \sum_{\ell=1}^L \alpha_\ell c(\phi_\ell, \beta_\ell) \exp(-j2\pi\tau_\ell f) + N(f) \quad (6)$$

with  $N(f)$  denoting a  $M$ -dimensional vector of complex white Gaussian noise and  $\theta = [\theta_1, \dots, \theta_L]$ . The contribution of the  $\ell^{\text{th}}$  wave to the channel transfer function is denoted as

$$S(f; \theta_\ell) = \alpha_\ell c(\phi_\ell, \beta_\ell) \exp(-j2\pi\tau_\ell f). \quad (7)$$

### 3. Estimation of Superimposed Signals using the SAGE Algorithm

#### 3.1 Maximum-Likelihood Estimation and the EM Algorithm

The problem to solve is the estimation of channel parameters, i.e., to obtain the  $L$  components of vector  $\theta$ . The maximum likelihood estimation (MLE) of this vector is computationally prohibitive owing to its high dimension when  $L$  is large and also because there is no closed formula

to express the maxima of the log-likelihood function used by the MLE. Even taking into consideration that the values of the complex amplitudes may be expressed as a function of the other parameters, the procedure to obtain the MLE represents a  $L$  3-D non-linear optimization process [9].

The EM algorithm [5] has been developed to address the MLE problem when a part of the observations is missing or suppressed. It is based on two key concepts: the *complete data* (unobservable) and the *incomplete data* (observable), allowing the decomposition of the above procedure in  $L$  3-D optimization procedures to estimate the waves' parameters, which may be performed separately and in parallel. Each 3-D optimization procedure aims to obtain the parameters of a given wave only. In our problem, a possible choice for the complete data set is the contribution of each individual wave to the channel transfer function, corrupted by a fraction of the additive noise, i.e.,

$$X_\ell(f) = S(f; \theta_\ell) + \sqrt{\mu_\ell} N(f) \quad (8)$$

where,  $\mu_\ell, \ell=1, \dots, L$ , must satisfy  $\sum \mu_\ell = 1$ . The vector containing the parameters of the  $\ell^{\text{th}}$  wave,  $\theta_\ell$ , constitutes one parameter subset. On the other hand, the measured (observed) channel transfer function,  $H(f)$ , represents the incomplete data set.

#### 3.2 Description of the SAGE Algorithm

The SAGE algorithm may be viewed as an extension of the EM algorithm: each one of the SAGE iterations is, in fact, an EM iteration to update just a subset of the components of  $\theta$ , maintaining the parameters of the other components fixed at their previous values. It replaces the  $L$  3-D parallel optimization procedures, used in the EM algorithm, by a serial optimization approach. As a result according to [4] and [9], in comparison to the EM algorithm, SAGE algorithm presents faster convergence and lower complexity. Although, according to [7] this may not be always true and the faster convergence can only be guaranteed if certain conditions are fulfilled. Again, the complete data set is chosen to be the contribution of each wave to the channel transfer function as given in (8) but choosing  $\mu_\ell=1$ . The  $L$  complete data sets,  $X_\ell(f), \ell=1, \dots, L$ , are independent, therefore the components  $X_{\ell'}, \ell' \neq \ell$  are of no importance for the estimation of  $\theta_\ell$ . The log-likelihood function of  $\theta_\ell$ , given an observation  $X_\ell(f) = X_\ell^{obs}(f)$ , is

$$\Lambda(\theta_\ell; X_\ell^{obs}) = 2 \int \Re \{ S^H(f'; \theta_\ell) X_\ell(f') \} df' - \int \| S^H(f'; \theta_\ell) \|^2 df' \quad (9)$$

where  $[ \cdot ]^H$  denotes the Hermitian operator. The MLE of  $\theta_\ell$  is given as

$$(\hat{\theta}_\ell)_{ML} (X_\ell^{obs}) \in \arg \max_{\theta_\ell} \{ \Lambda(\theta_\ell; X_\ell^{obs}) \} \quad (10)$$

where  $\hat{\theta}_\ell$  is the vector that contains the estimate of the  $\ell^{\text{th}}$  wave parameters.

Inserting (7) in (10) and approximating the integral by a sample summation, we may write

$$(\hat{\tau}_\ell, \hat{\phi}_\ell, \hat{\beta}_\ell)_{\text{ML}}(X_\ell^{\text{obs}}) = \arg \max_{[\tau, \phi, \beta]} \{ |z(\tau, \phi, \beta; X_\ell^{\text{obs}})| \} \quad (11)$$

$$(\hat{\alpha}_\ell)_{\text{ML}}(X_\ell^{\text{obs}}) = \frac{1}{MN} z((\hat{\tau}_\ell, \hat{\phi}_\ell, \hat{\beta}_\ell)_{\text{ML}}(X_\ell^{\text{obs}}); X_\ell^{\text{obs}})$$

with  $N$  the number of samples in the frequency domain and

$$z(\tau, \phi, \beta; X_\ell^{\text{obs}}) = c^{\text{H}}(\phi, \beta) X_\ell^{\text{obs}}(f) \exp(j2\pi f \tau). \quad (12)$$

Since all signals are superimposed on the available (measured) signal,  $X_\ell(f)$  cannot be observed, so we may try to obtain its estimate,  $\hat{X}_\ell(f; \hat{\theta}')$ , given the observation of  $H(f)$  and the previous estimate  $\hat{\theta}'$  of  $\theta$ . This can be done by removing the contribution of all waves, except the  $\ell^{\text{th}}$  wave, from the observation, i.e.,

$$\hat{X}_\ell(f; \hat{\theta}') = H(f) - \sum_{\substack{\ell'=1 \\ \ell' \neq \ell}}^L S(f; \hat{\theta}'). \quad (13)$$

Additional complexity reduction may be achieved, within the SAGE algorithm framework, by further decomposing the optimization procedure. Each subset  $\theta_\ell$  is split into three subsets:  $[\tau_\ell, \alpha_\ell]$ ,  $[\square_\ell, \alpha_\ell]$  and  $[\beta_\ell, \alpha_\ell]$  and the MLE is obtained for the parameters in each subset while maintaining the parameters in other sets fixed. As already mentioned, the MLE of  $\alpha_\ell$  may be expressed as a function of  $[\tau_\ell, \square_\ell, \beta_\ell]$ , so that the 3-D optimization procedure in (11) reduces to 3 1-D optimization procedures. The update procedures needed to obtain a new estimate for the parameters of the  $\ell^{\text{th}}$  wave,  $\hat{\theta}_\ell''$ , given the previous estimates of all waves,  $\hat{\theta}'$ , can then be written as

$$\hat{\tau}_\ell'' = \arg \max_{\tau} \{ |z(\tau, \hat{\phi}_\ell', \hat{\beta}_\ell'; \hat{X}_\ell(f; \hat{\theta}'))| \}, \quad (14)$$

$$\hat{\phi}_\ell'' = \arg \max_{\phi} \{ |z(\hat{\tau}_\ell'', \phi, \hat{\beta}_\ell'; \hat{X}_\ell(f; \hat{\theta}'))| \}, \quad (15)$$

$$\hat{\beta}_\ell'' = \arg \max_{\beta} \{ |z(\hat{\tau}_\ell'', \hat{\phi}_\ell'', \beta; \hat{X}_\ell(f; \hat{\theta}'))| \}, \quad (16)$$

$$\hat{\alpha}_\ell'' = \frac{1}{MN} z(\hat{\tau}_\ell'', \hat{\phi}_\ell'', \hat{\beta}_\ell''; \hat{X}_\ell(f; \hat{\theta}'))|. \quad (17)$$

Like in the original EM algorithm, the SAGE basic iteration stage that updates the parameters of a given wave comprises two steps: the E-step (Expectation), given in (13), aims to obtain the expected complete data set; and the M-step (Maximization), given in (11), performs the estimation of each parameter of the considered wave.

### 3.3 Initialization of the SAGE Algorithm

Beginning with the pre-initial setting  $\hat{\theta}' = [0, \dots, 0]$ , the initial estimates for each  $\ell=1, \dots, L$ , are obtained according to

$$\hat{\tau}_\ell'' = \arg \max_{\tau} \left\{ \sum_{m=1}^M |\hat{X}_\ell(f; \hat{\theta}') \exp(j2\pi f \tau)| \right\}, \quad (18)$$

$$(\hat{\phi}_\ell'', \hat{\beta}_\ell'') = \arg \max_{[\phi, \beta]} \{ |z(\hat{\tau}_\ell'', \phi, \beta; \hat{X}_\ell(f; \hat{\theta}'))| \} \quad (17)$$

and (17) to obtain  $\hat{\alpha}_\ell''$ .

In (18) the term inside the summation expresses frequency correlation. It is used as a method to obtain the initial delay estimate since at this point  $\hat{\phi}_\ell'$  and  $\hat{\beta}_\ell'$  are unknown. The 2-D optimization in (19) is used instead of (15) and (16) because according to [11] assuming  $\hat{\beta}_\ell' = 0$  may cause an erroneous azimuth estimation.

## 4. Results using Synthetic Data

Synthetic data have been generated using the extended Saleh-Valenzuela (ESV) model. The ESV model characterizes complex amplitude, time of arrival (ToA), angle of arrival (AoA) [1] and angle of departure (AoD) [13] for each multipath component (MPC). This model assumes that rays (or MPCs) arrive at the receiver in clusters and also that they have different statistical distributions for each of the parameters. If we discard de AoD, like in [1], the impulse response may be described by

$$h(\tau, \phi) = \sum_l \sum_k \alpha_{kl} \exp(j\psi_{kl}) \delta(\tau - T_l - \tau_{kl}) \delta(\phi - \Phi_l - \phi_{kl}) \quad (20)$$

where index  $l$  indicates the *cluster number* and index  $k$  indicates the *echo number within a cluster*.

The amplitude,  $\alpha_{kl}$ , follows a zero-mean Complex-Normal distribution whose deviation is described by an exponential decay with two time constants: one of them is associated to the clusters ( $\Gamma$ ) and the other to the rays within a cluster ( $\gamma$ ). The AoA follows a Laplacian distribution around a nominal cluster angle that is assumed to be uniformly distributed in the interval  $[0, 2\pi]$ . The ToA is modeled by a Poisson process with two arrival rates: again, one is associated to the clusters and other to the rays.

We aim to investigate the SAGE capability to retrieve the superimposed signals, that is: how the number of MPCs in the channel and their relative power influence the quality of the solution obtained. Thus, we have generated several sets of data with different combinations for number of clusters (NC) – number of rays in each cluster (NR) and also with different combinations for the time constants controlling the power decay ( $\Gamma$  and  $\gamma$ ). The arrival rates were the same for all sets. We have selected three of these

sets to present and the corresponding parameters, used in the ESV model, can be found in Tab. 1.

This data is then used to obtain the matrix of channel transfer functions which is computed according to (6) but without the added noise. We assumed: 801 frequency samples in a 200 MHz bandwidth centered on 2 GHz and a uniform rectangular array with 11 x 11 elements spaced by 0.5 λ in both dimensions. Some results may be observed in Fig. 1, Fig. 2 and Fig. 3.

Set Name	NC	NR	$\Gamma$ (ns)	$\gamma$ (ns)
ch3	5	10	60	20
ch4	3	5	90	30
ch9	5	10	120	40

Tab. 1. Parameters for the ESV model used to generate the data sets.

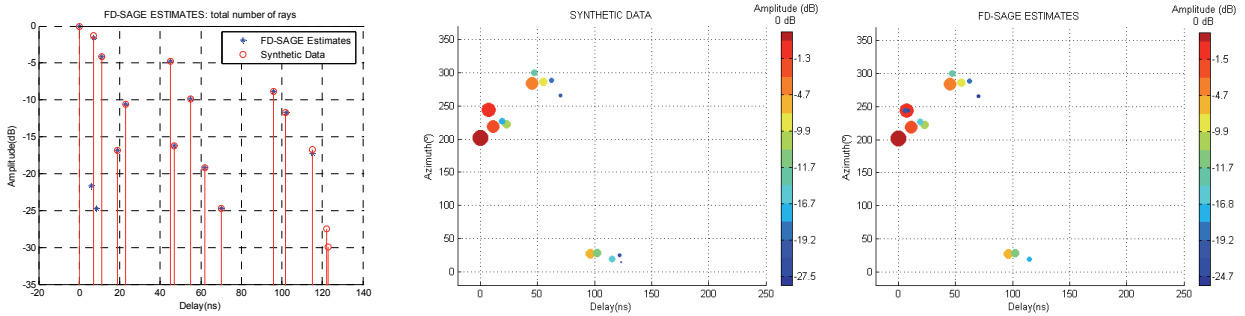


Fig. 1. SAGE retrieval results for a channel with 15 rays (ch4), moderate power decay and 15 estimates requested. **Left:** Generated impulse response and SAGE retrieval in time domain. **Center:** Generated impulse response. **Right:** SAGE retrieved impulse response. – Both in time and azimuth domains.

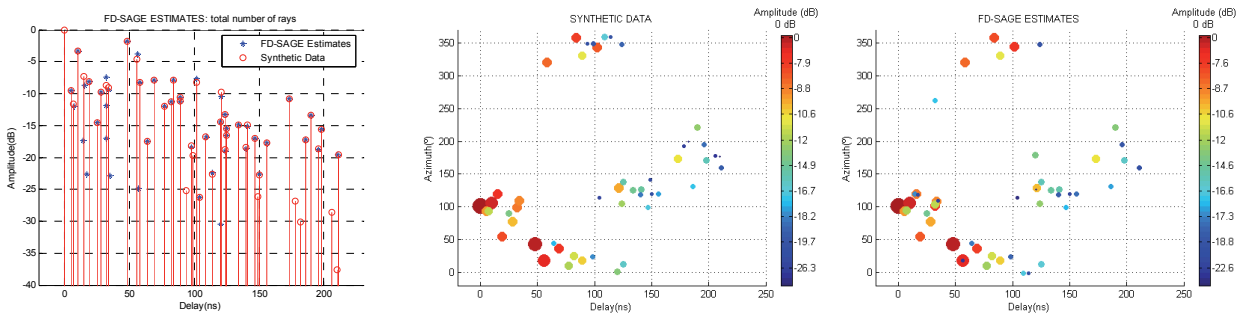


Fig. 2. SAGE retrieval results for a channel with 50 rays (ch9), moderate power decay and 15 estimates requested. **Left:** Generated impulse response and SAGE retrieval in time domain. **Center:** Generated impulse response. **Right:** SAGE retrieved impulse response. – Both in time and azimuth domains.

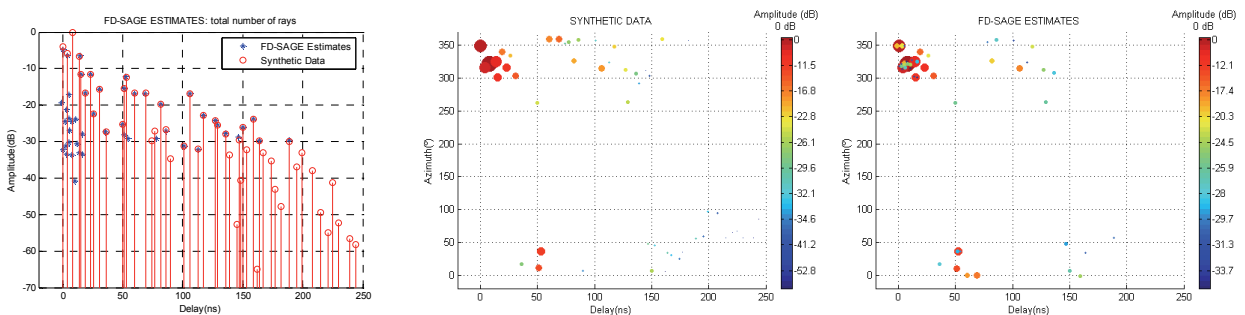


Fig. 3. SAGE retrieval results for a channel with 50 rays (ch3), pronounced power decay and 15 estimates requested. **Left:** Generated impulse response and SAGE retrieval in time domain. **Centre:** Generated impulse response. **Right:** SAGE retrieved impulse response. – Both in time and azimuth domains.

Observing the impulse responses of the sets presented here, we may conclude that in two of them – Fig. 1 and Fig. 2 – although the number of MPCs is very different, they present almost the same amplitude range (from 0 dB to about -30 dB) and in Fig. 3 the amplitude range is wider (from 0 dB to about -60 dB). Thus, we have classified the first two cases as “moderate” and the last one as “pronounced” power decay.

From the results shown we can conclude that if the channel presents a small number of rays and moderate power decay (Fig. 1), the SAGE algorithm is able to retrieve a good estimate for almost all the rays. In this particular case, notice that only the last two rays, which are simultaneously the weakest ones, were not correctly estimated. Instead, two inexistent and low amplitude rays are placed near the first and more powerful rays. Average delay and delay spread for the considered channel and the respective SAGE retrieval have been computed and compared. For this case errors were less than 1 % for both parameters, showing that, despite the failure in the estimation of those two rays, the retrieved waves represent a good description of this channel.

As the number of rays in the channel increases, the number of rays whose estimate is missed increases and therefore, the number of false rays retrieved also increases. In the case of Fig. 2, although the retrieved rays still provide a good description of the channel (average delay error of 1 % and delay spread error about 2.4 %), we have missed the estimate for 17 rays (out of a total of 50) and, obviously, there are 17 false echoes in the solution given by the algorithm. However, as the power decay becomes more pronounced the phenomenon also becomes more severe and thus, more evident. In the case of Fig. 3, the number of missed rays has increased to 24 (almost 50 % of the rays in the channel). Nevertheless, in general, the missed rays are the weakest ones so that the impact is not as bad as one could expect at first glance (for this case, average delay error is 3.2 % and delay spread error about 6 %).

## 5. Results on Real Channels

The measurement system, shown schematically in Fig. 4, consists of a 2D positioning device, driven by stepper motors, equipped with one antenna, a vector network analyzer (VNA) and a personal computer that is used to control the equipment, acquire and save experimental data. The VNA is used to measure the frequency response of the time-invariant channel at the  $M$  locations of a virtual rectangular antenna array. The computer controls the positioning device and the VNA through the use of a commercial stepper motor control card and a GPIB interface, respectively. The software needed to control all the equipment, acquire and save experimental data was implemented in LabVIEW.

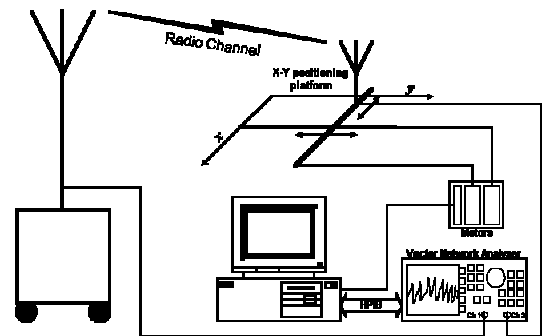


Fig. 4. Block diagram of the measurement system.

The frequency response of the time-invariant channel was measured at  $M=11 \times 11$  positions spaced by  $\lambda/2$  in both dimensions. The RF bandwidth was 200 MHz centered at 2 GHz. An elevated disconic antenna was used at the transmitter (Tx) location and a  $\lambda/4$  monopole antenna was used at the receiver (Rx) location. The monopole was moved along the  $M$  positions of the virtual rectangular antenna array. Fig. 5 shows the outdoor scenarios where the measurements presented below have taken place. The lines represent buildings with heights varying from 10 m to 15 m. The Tx height was about 7.5 m and the Rx height was about 1.3 m.

In order to obtain the parameters' estimates for a given number of waves, the matrix of frequency responses measured was used as input to the SAGE algorithm. Aiming the investigation on the algorithm's behavior, we must have a previous idea of the channel response to be able to judge the retrieved results. Therefore, in order to make such judgment, ray-tracing simulations were performed for the measurement scenarios and compared with the algorithm's results. This also provides us with the necessary insight to use the algorithm in situations in which we do not have a clear idea on the channel's response.

Nevertheless, we must bear in mind that results from ray tracing simulations may not be completely perfect. As a matter of fact, they depend on a rigorous description of the scenario dimensions and properties, the latter not always easy to obtain. Also, the more accurate are the results desired, the more complex and time consuming the simulation process will be, because it has to consider several physical phenomena (direct ray, reflection, diffraction, transmission). In fact, if we compare the simulated time domain impulse response of the channel (obtained by ray tracing tools) with the amplitude averaged time domain impulse response given by the measurements (obtained from the measured frequency response by applying an IFFT), sometimes we detect some simulated strong echoes at delays that are not present in the measured data and vice-versa.

The number of MPCs may be estimated, from observed data, by applying well-known information theoretic criteria, namely, the Akaike information criterion (AIC) and the minimum description length (MDL) [14], for

which several performance studies and improvements have been reported [15], [16], [17], since these were first proposed. Nevertheless, one must take into account the behavior presented by the SAGE algorithm in the previous section, showing that, even in the absence of noise, the algorithm misses some of the rays undergoing longer delays and supplies, in their place, false rays. As a result,

the number of rays to be requested from the SAGE algorithm,  $L$ , has been manually chosen by performing several attempts (trying different values) and analyzing the averaged time domain impulse response of the measured channel, the simulations and the output results of the SAGE algorithm. Results may be observed in Fig. 6 and Fig. 7.

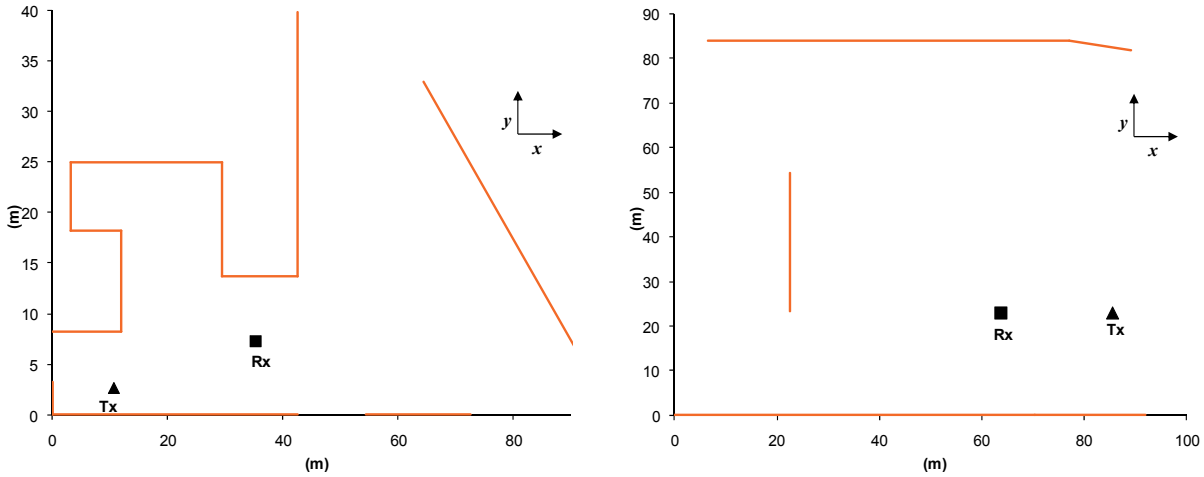


Fig. 5. Layouts of the measurement scenarios – Left: Ens5. Right: Ens6.

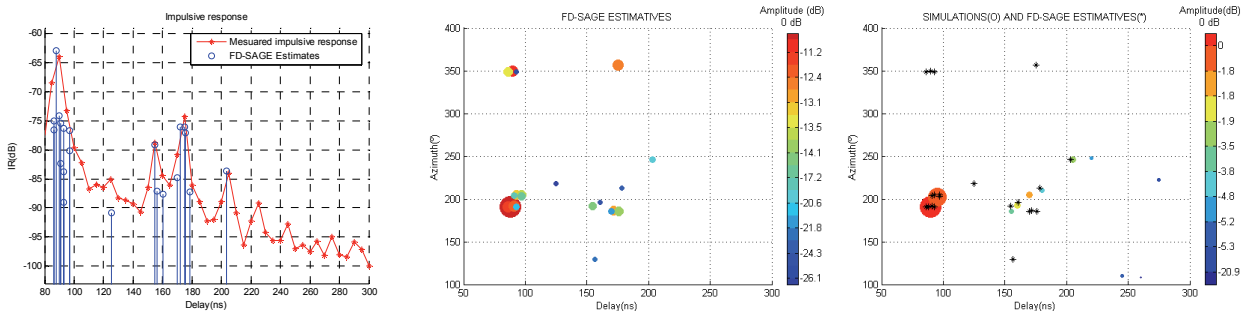


Fig. 6. Results for Ens5 with  $L = 21$ . Left: Measured channel and SAGE retrieved impulse responses (time domain). Centre: SAGE retrieved impulse response (time-azimuth domain). Right: Ray tracing simulations impulse response (time-azimuth domain).

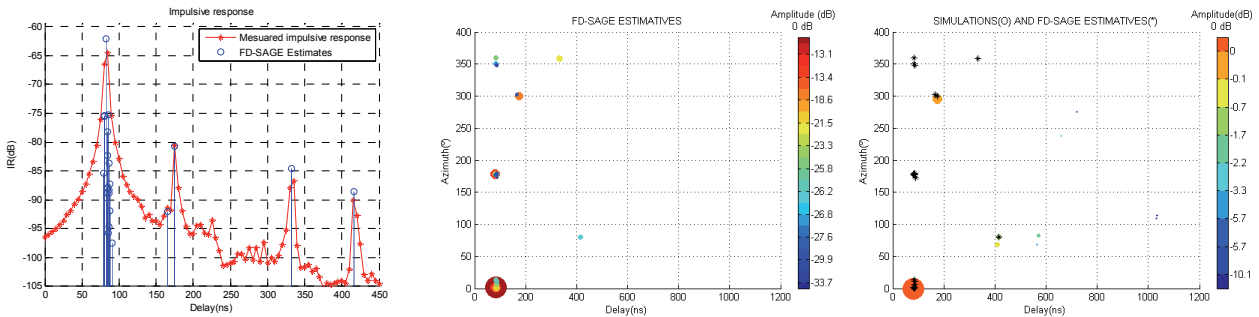


Fig. 7. Results for Ens6 with  $L = 23$ . Left: Measured channel and SAGE retrieved impulse responses (time domain). Centre: SAGE retrieved impulse response (time-azimuth domain). Right: Ray tracing simulations impulse response (time-azimuth domain).

The results in Fig. 6 and Fig. 7 were obtained by requesting the SAGE algorithm to provide estimates for 21 and 23 rays, respectively. We were able to retrieve almost all the contributions that are no more than about 25 dB below the strongest component. Again, we had computed the average delay and delay spread, using the measurements and the corresponding SAGE retrieval as well. When using the averaged time domain impulse response obtained from measurements, the computation has considered only the components which are no more than 25 dB below the highest peak. Averaged delays from SAGE retrieved data were within a maximum error of 0.3 % in agreement with the measured data, while for delay spreads, for the case of Fig. 6, we obtained an error of 5.8 % and for the case of Fig. 7, an error of 9.0 %, which are both reasonable.

## 6. Conclusions

This paper has dealt with the problem of estimating the parameters of a given number of superimposed signals using the SAGE algorithm. Ray retrieval results are presented both in synthetic channels, using data generated with the ESV model, and also in real channels.

From results in synthetic channels, we concluded that if the channel presents a small number of MPCs and moderate power decay, the SAGE algorithm is able to produce a good estimate for almost all MPCs. However, sometimes, the algorithm misses some of the most delayed MPCs and provides, in their place, some false MPCs. As the number of MPCs in the channel and the power decay increases, the number of MPCs whose estimate is missed increases and therefore, the number of false MPCs retrieved also increases. In general the missed MPCs are the weakest ones and thus, the impact is not as critical as one could expect.

The SAGE algorithm presents, in real channels, a similar behavior to the one presented with synthetic data. As a result, the number of rays that is requested from the algorithm must be carefully chosen. We must be aware that some of the outputted MPCs may be false and, if we do not have previous knowledge of the channel properties, we may not distinguish them easily. Nevertheless, false rays are likely to show parameters very similar to their neighbors, as if they were repeated.

## Acknowledgements

The authors would like to thank to the technicians from the Instituto de Telecomunicações for help with the measurements.

## References

- [1] SPENCER, Q. H., JEFFS, B. D., JENSEN, M. A., SWINDLEHURST, A. L. Modeling the statistical time and angle of arrival characteristics of an indoor multipath channel. *IEEE Journal on Selected Areas in Communications*, 2000, vol. 18, no. 3, p. 347 – 360.
- [2] STEINBAUER, M., MOLISCH, A. F., BONEK, E. The double-directional radio channel. *IEEE Antennas and Propagation Magazine*, 2001, vol. 43, no. 4, p. 51 – 63.
- [3] CHONG, C. C. *et al.* A new statistical wideband spatio-temporal channel model for 5-GHz band WLAN systems. *IEEE Journal on Selected Areas in Communications*, 2003, vol. 21, no. 2, p. 139 – 150.
- [4] FESSLER, J. A., HERO, A. O. Space-alternating generalized expectation-maximization algorithm. *IEEE Transactions on Signal Processing*, 1994, vol. 42, no. 10, p. 2664 – 2677.
- [5] FEDER, M., WEINSTEIN, E. Parameter-estimation of superimposed signals using the EM algorithm. *IEEE Transactions on Acoustics Speech and Signal Processing*, 1988, vol. 36, no. 4, p. 477 – 489.
- [6] FESSLER, J. A., HERO, A. O. Penalized maximum-likelihood image-reconstruction using space-alternating generalized EM algorithms. *IEEE Transactions on Image Processing*, 1995, vol. 4, no. 10, p. 1417 – 1429.
- [7] CHUNG, P. J., BOHME, J. F. Comparative convergence analysis of EM and SAGE algorithms in DOA estimation. *IEEE Transactions on Signal Processing*, 2001, vol. 49, no. 12, p. 2940 – 2949.
- [8] CHUNG, P. J., BOHME, J. F. Experimental study of the EM and SAGE algorithms with application to sonar data. In *Sensor Array and Multichannel Signal Processing Workshop Proceedings*. Rosslyn (USA), 2002, p. 77 – 81.
- [9] FLEURY, B. H., TSCHUDIN, M., HEDDERGOTT, R., DAHLHAUS, D., PEDERSEN, K. I. Channel parameter estimation in mobile radio environments using the SAGE algorithm. *IEEE Journal on Selected Areas in Communications*, 1999, vol. 17, no. 3, p. 434 – 450.
- [10] CHONG, C. C. *et al.* Joint detection-estimation of directional channel parameters using the 2-D frequency domain SAGE algorithm with serial interference cancellation. In *ICC 2002, IEEE International Conference on Communications*, vol. 2. New York (USA), 2002, p. 906 – 910.
- [11] TSCHUDIN, M., HEDDERGOTT, R., TRUFFER, P. Validation of a high resolution measurement technique for estimating the parameters of impinging waves in indoor environments. In *Ninth IEEE International Symposium on Personal, Indoor and Mobile Radio Communications*. Boston (USA), 1998, p. 1411 – 1416.
- [12] MOTA, S., ROCHA, A. Parameter estimation of synthetic and real radio channels using the SAGE algorithm. In *13<sup>th</sup> IEEE International Symposium on Personal, Indoor and Mobile Radio Communications Proceedings - Sailing the Waves of the Wireless Oceans*. Lisboa (Portugal), 2002, p. 634 – 638.
- [13] WALLACE, J. W., JENSEN, M. A. Modeling the indoor MIMO wireless channel. *IEEE Transactions on Antennas and Propagation*, 2002, vol. 50, no. 5, p. 591 – 599.
- [14] WAX, M., KAILATH, T. Detection of signals by information theoretic criteria. *IEEE Transactions on Acoustics Speech and Signal Processing*, 1985, vol. 33, no. 2, p. 387 – 392.

- [15] ZHANG, Q. T., WONG, K. M., YIP, P. C., REILLY, J. P. Statistical analysis of the performance of information theoretic criteria in the detection of the number of signals in array processing. *IEEE Transactions on Acoustics, Speech and Signal Processing*, 1989, vol. 37, no. 10, p. 1557 – 1567.
- [16] FISHLER, E., GROSMANN, M., MESSER, H. Detection of signals by information theoretic criteria: general asymptotic performance analysis. *IEEE Transactions on Signal Processing*, 2002, vol. 50, no. 5, p. 1027 – 1036.
- [17] NADLER, B. Nonparametric detection of signals by information theoretic criteria: performance analysis and an improved estimator. *IEEE Transactions on Signal Processing*, 2010, vol. 58, no. 5, p. 2746 – 2756.

### About Authors ...

**Susana MOTA** was born in Anadia, Portugal. She received her B.Sc. (5 years course) and M.Sc. degrees from the University of Aveiro, Portugal, both in electronics and telecommunications, in 1999 and 2003, respectively. Currently she is working towards the Ph.D. degree at the same university where she is also an invited lecture at the Department of Electronics, Telecommunications and Informatics. Her research interests are in wireless communications, directional channel characterization and MIMO channel modeling. She is member of EU COST IC0802 action.

**Maura OUTEIRAL GARCIA** was born in Boiro, Spain. During this work, she was an ERASMUS student on a leave from University of Vigo, Spain, working towards the M.Sc. degree in telecommunications, at University of Aveiro, Portugal. She has been involved in wireless

channel propagation, mainly concerning, directional channel characterization and clustering algorithms.

**Armando ROCHA** was born in Laguaira, Venezuela. He obtained his degree in telecommunication and electronics Engineering in 1984 from the University of Aveiro and his PhD from the same university in 1996. He is an auxiliary professor at the Department of Electronics, Telecommunications and Informatics at the same university. He lectures in wave propagation, guided propagation, antennas and cellular planning. He has been involved in Earth-Satellite microwave propagation activities developing beacon receivers, doing propagation measurements and channel modeling. He was in Management Committee Member of EU COST 280 and currently participates with the same role in COST IC0802. He also participated in several public funded projects.

**Fernando PEREZ FONTAN** was born in Villagarcía de Arosa, Spain. He obtained his degree in telecommunication engineering in 1982 from the Technical University of Madrid and his PhD in 1992 from the same university. After working in industry since 1984 he became an assistant professor at the University of Vigo in 1988. In 1993 he became an associate professor and in 1999 a full professor at the Signal Theory and Communications Department of the University of Vigo. He lectures in Radiocommunication Systems, especially in terrestrial fixed and mobile system related topics. He is the author of a number of books and journal papers and has been the leader in several projects funded by public and private entities. He participates in ITU-R WG3 on Propagation Modeling. He has been a Management Committee Member of EU' COST 255, 280 and 297, and currently participates with the same role in COST IC0802.